Cumhuriyet Science Journal

e-ISSN: 2587-246X
ISSN: 2587-2680

Cumhuriyet Sci. J., 42(3) (2021) 715-721
http://dx.doi.org/10.17776/csj.923274

Magnetic phase transitions due to compositional variation across amorphous thin–films

Mustafa TOKAÇ [1,*]

[1]*Alanya Alaaddin Keykubat University, Faculty of Engineering, Department of Fundamental Sciences, Antalya/TURKEY*

Abstract

The structural and magnetic properties of amorphous thin–films with various CoFeTaB thicknesses were studied to observe magnetic phase transitions due to compositional variation through the CoFeTaB layer. The investigations of the structural properties of amorphous CoFeTaB thin–films were undertaken to confirm layer thickness, interface roughness, and their amorphous structure. Temperature dependent magnetic characterizations were performed to extract Curie temperatures of each thin–film structure, where there is evidence of more than one magnetic transition point. These transition points indicate magnetic phase transitions, which may be attributed to compositional variations across the amorphous CoFeTaB thin–films. Investigation of diffusion process in ferromagnetic thin–films is crucial for the development of spintronic applications.

Article info

History:
Received:19.05.2021
Accepted:03.07.2021

Keywords:
Fe–based amorphous alloys,
Magnetic properties,
Ferromagnetic thin–films,
Magnetic phase transitions.

1. Introduction

High–moment ferromagnetic CoFe alloys show excellent soft magnetic properties, including high saturation magnetization, high spin polarization, and low coercivity, and they have been considered to have considerable potential for use in many technological applications in the fields of spintronics [1–3]. CoFe alloy has a BCC crystal structure with a cubic magnetocrystalline anisotropy. The addition of B of composition greater than 20% in the CoFe alloy produces an amorphous metallic glass with a reduced Curie temperature (T_C) and reduced magnetization compared to CoFe alloy [4]. Amorphous ferromagnetic alloys represent an important class of materials, which have a unique disorder atomic arrangements and zero magnetocrystalline anisotropy energy, which makes amorphous metallic alloys functional for a broad range of applications. Amorphous CoFeB thin–films have been attracted extensive attention in recent years in giant and tunnelling magnetoresistance devices [5,6], current–induced magnetization switching [7], and are utilized in commercial applications such as HDD read–heads and magnetic random access memories. The amorphous CoFeB alloys have high spin polarization, which could lead to a high TMR value at room temperature [5,6]. The addition of a transition metal to an amorphous Fe–based alloy, reduces both the T_C and the magnetic moment per Co and Fe atoms [8], where this reduction can be explained as a result of charge transfers from the transition metal atoms to the unfilled holes in the electronic d–states of the Fe.

The discovery of the perpendicularly magnetized Ta/CoFeB/MgO heterostructures, which exhibit perpendicular magnetic anisotropy (PMA) is attracting significant interest for potential applications in magnetic random access memory (MRAM) [6]. The underlayer to the CoFeB layer also plays a crucial role in the size of PMA, where Ta is widely used as an underlayer because the Ta/CoFeB interface can control the perpendicular magnetic anisotropy and the related magnetic responses [9]. Diffusion of Fe atoms towards oxide layer has been reported in CoFeB/MgO structures during the deposition of MgO, where a Fe–O rich interfacial region was formed with reduced magnetization [10]. Another study showed that T_C can be tuned from 200 K to below 100 K by increasing Ta composition from ~ 15% to ~30% in FeTa amorphous alloy [8]. In order to identify the influence of the Ta diffusion in the magnetic properties of the ferromagnetic layer, the relationship between the structural and magnetic properties of this structure needs to be clarified. The influence of the diffusion of Ta in the Ta/CoFeB/MgO system has often been discussed [11–13], however, there is no sufficient information that clearly shows the relationship between the Ta diffusion and the magnetic properties of a ferromagnetic layer at low temperatures.

*Corresponding author. *e-mail address: mustafa.tokac@alanya.edu.tr.*
 ©2021 Faculty of Science, Sivas Cumhuriyet University

Previously, Ta diffusion within the CoFeTaB layer has been observed during the thin–film deposition, which causes variation of magnetization and T_C through the thin–film [14]. As many spintronic devices work at elevated temperatures, understanding the Ta diffusion on the magnetic properties of CoFeTaB thin–film is important for the development of spintronic applications. The amorphous CoFeTaB alloy used in this study was designed to have a T_C below room temperature in order to observe the influence of Ta diffusion on the magnetic properties at low temperatures. In this manuscript, the structural and magnetic properties of the bilayered amorphous thin–film with various CoFeTaB thicknesses were studied to indicate magnetic phase transitions due to Ta diffusions at low temperatures because diffusion of Ta produces regions of different composition through the CoFeTaB layer, which causes variation of magnetization and T_C through thin–films.

2. Experimental Procedures

In this study, a series of amorphous ferromagnetic thin–films ($Co_{30}Fe_{30}Ta_{25}B_{15}$ – The subscript represents the nominal composition of CoFeTaB) with a thickness from 10 Å to 40 Å were deposited at room temperature onto Si (100) substrate using dc magnetron sputtering under ultra–high vacuum. The structure of the layer stacks was Si/SiO_2/CoFeTaB (t)/Ta(30 Å)/Ta_2O_5 with a CoFeTaB layer thickness ranging from 10 to 40 Å, as shown schematically inset of Figure 1a. The $Co_{30}Fe_{30}Ta_{25}B_{15}$ layers (CoFeTaB hereafter) were capped with a 30 Å Ta layer to prevent oxidation. Grazing incidence x–ray reflectivity (XRR) was performed using a Rigaku Smartlab laboratory reflectometer at room temperature in order to characterize the physical structure of each thin–film. X–ray reflectivity scans were performed by scanning $\theta - 2\theta$ from 0° to 6° with a step size of 0.02°. All reflectivity measurements were fitted using the GenX simulation code [15], which utilizes the Parratt recursive formalism for simulating specular reflectivity. It uses a model based on the sample structure including free structural parameters to determine the layer thickness and interface/surface roughness and densities of each layer. In order to validate the amorphous nature of the CoFeTaB films, x–ray diffraction (XRD) profiles were obtained. Magnetic characterization of amorphous CoFeTaB thin–films was performed using a Quantum Design superconducting quantum interference device (SQUID) magnetometry in a temperature range between 5 K to 300 K with an external magnetic field of 100 Oe to extract T_C for each thin–films.

3. Results and Discussion

3.1. Structural characterization of thin–films

Measured grazing incidence XRR data and corresponding best fit simulations for 40 Å CoFeTaB thin–film are presented in Figure 1a. Here, the red solid line represents simulated fits of specular reflectivity data. Reflectivity simulations were performed by starting with nominal thicknesses of each layer of the as–deposited thin–films and adding a thin Ta_2O_5 layer to model oxide formation on the Ta cap, with a thickness up to a few nanometers. To improve the fitting quality of the XRR data, a thermally oxidized SiO_2 layer on top of the Si (100) substrate was added. The structural parameters including layer thicknesses, interface roughnesses, and layer densities were obtained from the best–fitting simulations of amorphous thin–films as a function of CoFeTaB thicknesses. Sample parameters from best fit XRR including layer thickness and interface roughness used in the simulation of specular reflectivity of amorphous thin–films with various CoFeTaB thickness are summarized in Table 1. It is well–known that surface/interface roughness affects the magnetic properties of thin–film structures, such as domain structure, and magnetic anisotropy [16], where it has been shown that an increase in interface roughness increases the exchange bias field and the coercivity [17]. The roughness parameters for each structure are around 3 Å, indicating thin–films are continuous in the direction normal to the scattering plane.

The structural characterization of thin–films was undertaken using an x–ray diffraction (XRD) pattern to derive information on the nature of the crystal structure. Figure 1b presents the XRD patterns of all thin–films with various CoFeTaB thicknesses studied here. As shown in the figure, all thin–films revealed an XRD peak at 2θ of 69° corresponding to the (400) diffraction peak of the Si (100) substrate. The Bragg peaks corresponding to all CoFeTaB thin–films are not observed in these patterns which confirm the amorphous nature of CoFeTaB layers.

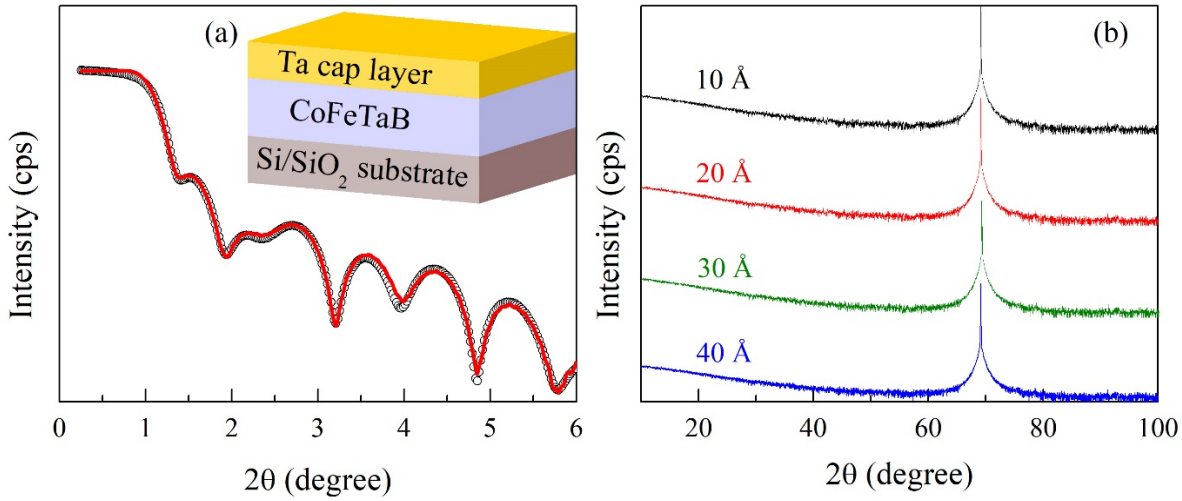

Figure 1: (a) Specular reflectivity data and corresponding simulated reflectivity for amorphous 40 Å CoFeTaB thin–film. The red solid line represents best–fit simulations. The inset shows the sample schematic. (b) X–ray diffraction pattern of the amorphous thin–films with various CoFeTaB thicknesses.

The structural scattering length density (SLD) profiles and their derivatives for all structures are given in Figure 2 for thin–films with various CoFeTaB thicknesses, as shown by shaded regions. Here, the width of the substrate/CoFeTaB interface appears relatively broad for all thin–films. This broad interface is attributed to the diffuse interface between the Si (100) substrate and the thin SiO_2 layer. Within the volume of the CoFeTaB films, the structural SLDs are roughly constant, which indicates the ferromagnetic CoFeTaB layers are uniform layers. However, the structural SLD profiles are varied from the bulk values in the interface of the CoFeTaB/Ta capping layer, which suggests that compositionally–graded layers are formed in the region of CoFeTaB layers and the Ta capping layers. During the deposition of thin–films, the interdiffusion of Ta atoms into CoFeTaB layers is possible because highly energetic Ta atoms can penetrate into the CoFeTaB layer, resulting in a broad CoFeTaB/Ta structural interface. Interdiffusion of atoms has studied at CoFeB/Ta and CoFeB/Ru interfaces, where Ta atoms can penetrate more deeply into the CoFeB layer because Ta is heavier than Ru [18]. A similar study has shown that a 0.2 nm thick TaB layer is formed at CoFeB/Ta interface after annealing of CoFeB/Ta thin–films, which is due to out–diffusion of B atoms from the CoFeB layer to the Ta capping layer [19].

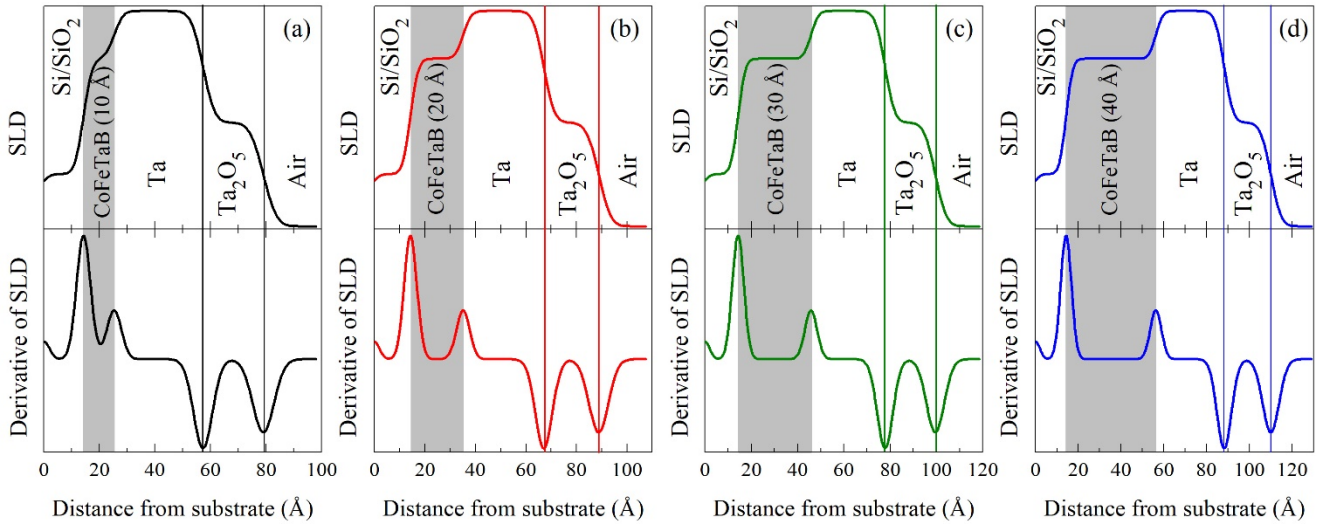

Figure 2: Structural scattering length density profiles and their derivatives for amorphous thin–films. The shaded regions show with various CoFeTaB layer thicknesses ranging from 10 to 40 Å. The vertical dashed lines correspond to the positions of the layer interfaces in the model structures.

The derivatives of the structural SLD profiles are plotted in Figure 2 to visualize positions of the structural interfaces more accurately in these structures with various CoFeTaB thicknesses. Here, the peaks and dips show each layer interfaces in the model structures, shown by vertical solid lines. In the derivative of SLDs, the first peaks correspond to the thickness of ~ 15 Å for both structures which indicates the thickness of the SiO_2 layer, and beyond this thickness, the magnetic CoFeTaB layer starts to increase. The second peaks, indicating CoFeTaB/Ta interface, shift to the right as the thickness of the CoFeTaB layer increases. The shaded regions indicate the approximate thickness of CoFeTaB layers and the vertical solid lines correspond to the approximate positions of the layer interfaces in the model structures.

3.2. Magnetic characterization of thin–films

The main purpose of the present study is the investigation of the magnetic phase transitions for thin–films with various CoFeTaB thicknesses, as given in Figure 3. Here, the magnetic response of thin–films shows that the CoFeTaB layers do not act as a single homogeneous magnetic layer with a single T_C, as usual. Instead, the ferromagnetic layers comprise two or three magnetic sub–layers depending on layer thicknesses. These inhomogeneities are related to the Ta distribution within the CoFeTaB layer, as it varies the T_C, resulting in the asymmetry in magnetic properties at the CoFeTaB/Ta interface, and indicating the contribution of the different moments at the CoFeTaB/Ta interface and within the CoFeTaB layer. At low temperatures, the temperature dependent magnetization in a ferromagnetic material can be fitted using the spin–wave model and described by the Bloch $T^{3/2}$ power–law equation given as,

$$M(T) = M(0)\left[1 - \left(\frac{T}{T_C}\right)^{3/2}\right] \qquad (1)$$

where M(0) is the spontaneous magnetization at absolute zero. The spontaneous magnetization approaches zero when the temperature increases towards the T_C and phase transition from paramagnetic to ferromagnetic state is observed, which is identified as a point of abrupt change in magnetic behaviour. In order to understand the magnetic phase transitions due to Ta diffusion within the CoFeTaB layer, there is evidence of more than one transition point, notated as T_C's in the magnetic behavior of thin–films. Therefore, it is quite difficult to obtain T_C values from temperature dependent magnetization profiles using Equation (1).

The derivative of temperature dependent magnetization curves for all thin–film structures with various CoFeTaB thicknesses are calculated. The curves, where the derivative of magnetization reaches a minimum value, indicate more than one transition point in the magnetic response, as noted T_C's for all thin–film structures. Two phase transitions are observed, indicating two different magnetic regions, denoted as T_{C1} and T_{C2}, across the thin–film with 10 Å CoFeTaB thickness. For the rest of the thin–films, there are three transition temperatures, denoted as T_{C1}, T_{C2}, and T_{C3}, indicating three active magnetic regions. These transition points show magnetic phase transitions, which may be attributed to compositional variations across the CoFeTaB thin–films. These variations suggest non–uniformity in the magnetic profile due to the Ta distribution in the CoFeTaB layer, causing variations in the T_C's.

Figure 3a shows temperature–dependent magnetization and its derivative for the thin–film with 10 Å CoFeTaB thickness. The derivative of magnetization shows two sharp curves, which indicate magnetic phase transitions at temperatures as shown by T_{C1} and T_{C2}, where these transitions are at ~ 220 K and ~ 50 K, respectively. The thinnest CoFeTaB film might have adopted the Volmer–Weber growth mode on SiO_2, where the vaporized atoms bond to each other more strongly than to the substrate surface. This strong bonding leads to the formation of islands that join to form continuous thin–film structures. The coverage of the CoFeTaB layer at 10 Å may not be 100%, hence the Ta capping layer grown on top of CoFeTaB will have a lesser CoFeTaB neighbor. As a result of this low CoFeTaB thickness, Ta atoms may be in direct contact with the substrate surface, which may create compositional variations in the magnetic response of the CoFeTaB layer. This results in two magnetic phase transitions, where T_{C1} is the first transition temperature at 220 K, attributed to the magnetic region adjacent to the

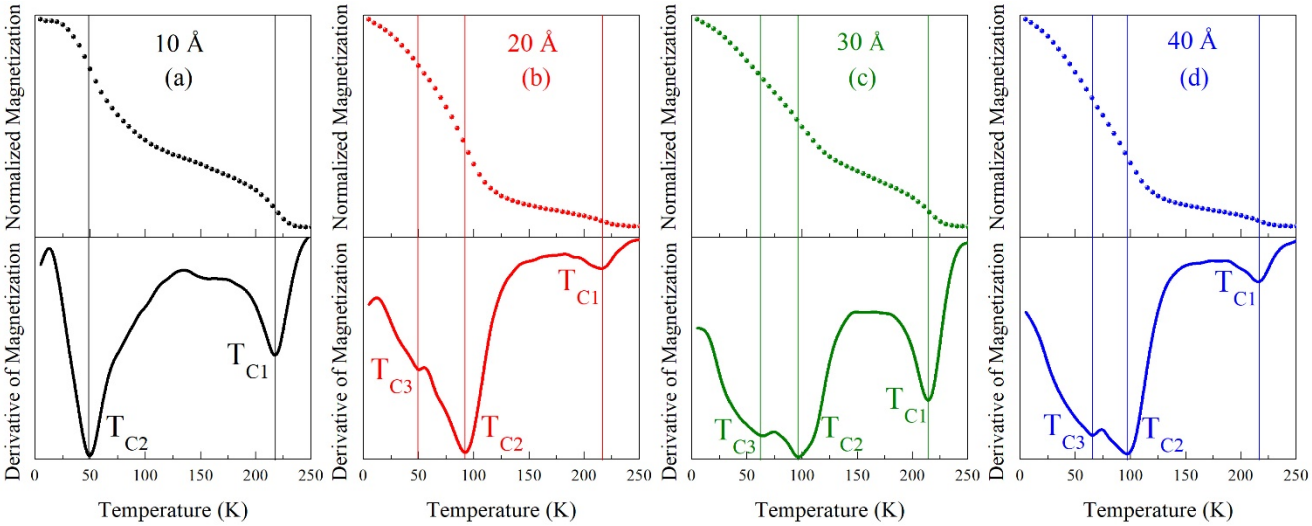

Figure 3: Temperature dependence of magnetization curves and their derivatives for amorphous thin–films with various CoFeTaB thicknesses measured under the magnetic field of 100 Oe.

buffer interface with less Ta concentration, and T_{C2} is the second transition temperature at 50 K, attributed to the magnetic region adjacent to the top interface with the maximum Ta concentration, the least magnetic moment and the lowest T_{C2}.

An increase in the thickness of the CoFeTaB layer leads to a better surface coverage due to the coalescence of grains, causing multiple phase transitions across CoFeTaB layers. As the thickness of the CoFeTaB layer increases to 20 Å, as shown in Figure 3b, the magnetization appears relatively broad at temperatures between 125 K to 225 K, and a magnetic phase transition is observed at $T_{C1} \sim 220$ K. This is attributed to the transition temperature of the sublayer with less Ta concentration, corresponding to a magnetic region adjacent to the buffer interface. A second transition point is observed more clear, as shown by the sharp curve on the derivative of magnetization at $T_{C2} \sim 90$ K. The T_{C2} may be the transition temperature of the magnetic thin–slab at the center of the CoFeTaB layer because heavy Ta atoms can penetrate within the center of the CoFeTaB layer during the deposition of the Ta capping layer. Also, a third transition point, which is not clear as others, emerges slightly indicated by $T_{C3} \sim 50$ K, which may be the transition temperature of a magnetic region adjacent to the top interface, with the lowest transition temperature and the highest Ta concentration.

Similar transition temperatures are obtained as $T_{C1} \sim 220$ K, $T_{C2} \sim 95$ K, and $T_{C3} \sim 65$ K for the rest of the thin–films, as given in Figure 3c and 3d. Here, T_{C1} has the same transition temperature as for the films with 10 Å and 20 Å CoFeTaB thicknesses. This is attributed to the transition temperature of the magnetic region close to the bottom interface with less Ta concentration. The second transition temperature $T_{C2} \sim 95$ K, corresponds to the magnetic thin–slab at the center of the CoFeTaB layer with the higher Ta concentration compared to the magnetic region at the buffer interface. $T_{C3} \sim 65$ K, is the third transition temperature of the magnetic slab adjacent to the Ta capping layer, where the maximum Ta concentration at this thin–slab causes the reduction of T_C. All transition temperatures of each thin-film structures are summarized in Table 1.

10 nm thick CoFeTaB thin–film with 30% Ta concentration, sandwiched with 3 nm thick Pt layers was studied to understand the temperature dependent interfacial magnetization, where diffusion of Ta creates magnetic regions of different composition and resulting in three different transition temperatures. These transition temperatures were obtained as $T_{C1} \sim 215$ K, $T_{C2} \sim 120$ K, and $T_{C3} \sim 80$ K, where T_{C1} and T_{C2} correspond to the transition temperature of the region adjacent to the bottom/top interfaces, respectively. $T_{C3} \sim 80$ K indicates the transition point of the center of the CoFeTaB layer with the highest Ta concentration and least magnetic moment, which is attributed to the the transition temperature from paramagnetic to ferromagnetic state [20]. As it is known

Table 1: Sample parameters from best fit XRR including layer thickness and interface roughness used in the simulation of specular reflectivity of amorphous CoFeTaB thin–films, and transition temperatures, obtained from the minimum value of the derivative of magnetization.

Sample	Layer	Thickness (Å)	Roughness (Å)	Transition Temperatures (K)		
				T_{C1}	T_{C2}	T_{C3}
CoFeTaB (10 Å)	CoFeTaB	10.5 ± 0.8	2.4 ± 1.2	220	50	---
	Ta	31.5 ± 3.3	3.3 ± 1.3			
CoFeTaB (20 Å)	CoFeTaB	21.1 ± 1.4	2.1 ± 1.2	220	90	50
	Ta	32.3 ± 1.8	3.4 ± 1.7			
CoFeTaB (30 Å)	CoFeTaB	30.9 ± 1.6	2.3 ± 1.5	220	95	65
	Ta	31.8 ± 2.5	3.1 ± 1.8			
CoFeTaB (40 Å)	CoFeTaB	41.2 ± 2.3	2.4 ± 1.2	220	95	65
	Ta	30.9 ± 2.5	2.6 ± 1.5			

that higher Ta concentration decreases the T_C and the magnetic moment per Co and Fe atoms [8], it is also possible to comment about the location of transition temperatures for each magnetic region in this study. In the present work, similar behaviour of magnetic transition temperatures is obtained for CoFeTaB/Ta bilayered thin–films. Due to the compositional variation of Ta (30%) through the ferromagnetic layer, the T_C was estimated as ~ 80 K [20], which is 15 K lower than the T_C of 30 Å and 40 Å thick CoFeTaB thin–films studied here. The transition temperature of T_{C1} is obtained as ~ 220 K for all thin – film structures, which indicates the initial stage of the deposition for all thin–films show similar behaviour and resulting in the magnetic thin–slab adjacent to the buffer interface. These phase transitions confirm the expected compositional variations within the CoFeTaB layers.

4. Conclusion

In summary, the magnetic phase transitions due to compositional variation of the Ta capping layer were studied for amorphous thin–films with various CoFeTaB thicknesses. An investigation of the structural properties of amorphous thin–films was undertaken to confirm layer thickness, interface roughness, and the amorphous structure of thin–films. Temperature dependent magnetic characterizations were performed to extract Curie temperatures of each thin–film, where the CoFeTaB layer does not act as a homogenous magnetic layer with a single T_C. Instead, the data suggest more than one magnetic transition point, which indicates multiple magnetic phase transitions. These transitions may be attributed to compositional variations through the amorphous CoFeTaB layer thickness.

Acknowledgement

The author acknowledges Dr. A. T. Hindmarch and Dr. C. J. Kinane for their assistance with film preparation and experimental work.

Conflicts of interest

The author states that there is no conflict of interests

References

[1] Cooper E. I., Bonhote C., Heidmann J., Hsu Y., Kern P., Lam J. W., Ramasubramanian M., Robertson N., Romankiw L. T., Xu H., Recent developments in high-moment electroplated materials for recording heads, *IBM Journal of Research and Development,* 49 (1) (2005) 103-126.

[2] Chen A. P., Burton J. D., Tsymbal E. Y., Feng Y. P., Chen J., Effects of B and C doping on tunneling magnetoresistance in CoFe/MgO magnetic tunnel junctions, *Physical Review B,* 98 (4) (2018) 045129.

[3] Parkin S. S., Kaiser C., Panchula A., Rice P. M., Hughes B., Samant M., Yang S. H., Giant tunnelling magnetoresistance at room temperature

with MgO (100) tunnel barriers, *Nature Materials*, 3 (12) (2004) 862-867.

[4] Platt C. L., Minor N. K., Klemmer T. J., Magnetic and structural properties of FeCoB thin films, *IEEE Transactions on Magnetics,* 37 (4) (2001) 2302-2304.

[5] Djayaprawira D. D., Tsunekawa K., Nagai M., Maehara H., Yamagata S., Watanabe N., Yuasa S., Suzuki Y., Ando K., 230% room-temperature magnetoresistance in CoFeB/MgO/CoFeB magnetic tunnel junctions, *Applied Physics Letters,* 86 (9) (2005) 092502.

[6] Ikeda S., Miura K., Yamamoto H., Mizunuma K., Gan H. D., Endo M., Kanai S., Hayakawa J., Matsukara F., Ohno H., A perpendicular-anisotropy CoFeB–MgO magnetic tunnel junction, *Nature Materials,* 9 (9) (2010) 721-724.

[7] Kubota H., Fukushima A., Yakushiji K., Nagahama T., Yuasa S., Ando K., Maehara H., Nagamine Y., Tsunekawa K., Djayaprawira D. D., Watanabe N., Suzuki Y., Quantitative measurement of voltage dependence of spin-transfer torque in MgO-based magnetic tunnel junctions, *Nature Physics,* 4 (1) (2008) 37-41.

[8] Fukamichi K., Gambino R. J., The Curie temperature and magnetization of Fe-base amorphous binary alloys containing transition metal, *IEEE Transactions on Magnetics,* 17 (6) (1981) 3059-3061.

[9] Cheng C.-W., Feng W., Chern G., Lee C. M., Wu T.-H., Effect of cap layer thickness on the perpendicular magnetic anisotropy in top MgO/CoFeB/Ta structures, *Journal of Applied Physics,* 110 (3) (2011) 033916.

[10] Hindmarch A. T., Dempsey K. J., Ciudad D., Negusse E., Arena D. A., Marrows C. H., Fe diffusion, oxidation, and reduction at the CoFeB/MgO interface studied by soft x-ray absorption spectroscopy and magnetic circular dichroism, *Applied Physics Letters,* 96 (9) (2010) 092501.

[11] Ikeda S., Hayakawa J., Ashizawa Y., Lee Y. M., Miura K., Hasegawa H., Tsunoda M., Matsukura F., Ohno H., Tunnel magnetoresistance of 604% at 300 K by suppression of Ta diffusion in CoFeB/MgO/CoFeB pseudo-spin-valves annealed at high temperature, *Applied Physics Letters,* 93 (8) (2008) 082508.

[12] Wang W. X., Yang Y., Naganuma H., Ando Y., Yu R. C., Han X. F., The perpendicular anisotropy of Co40Fe40B20 sandwiched between Ta and MgO layers and its application in CoFeB/MgO/CoFeB tunnel junction, *Applied Physics Letters,* 99 (1) (2011) 012502.

[13] Worledge D. C., Hu G., Abraham D. W., Sun J. Z., Trouilloud P. L., Nowak J., Brown S., Gaidis M. C., O'Sullivan E. J., Robertazzi R. P., Spin torque switching of perpendicular Ta|CoFeB|MgO-based magnetic tunnel junctions, *Applied Physics Letters,* 98 (2) (2011) 022501.

[14] Tokaç M., Kinane C. J., Atkinson D., Hindmarch A. T., Temperature dependence of magnetically dead layers in ferromagnetic thin-films, *AIP Advances,* 7 (11) (2017) 115022.

[15] Björck M., Andersson G., GenX: an extensible X-ray reflectivity refinement program utilizing differential evolution, *J. Appl. Crystallogr.,* 40 (6) (2007) 1174-1178.

[16] Zhang S., Levy P. M., Enhanced spin-dependent scattering at interfaces, *Physical Review Letters,* 77 (5) (1996) 916.

[17] Fleischmann C., Almeida F., Demeter J., Paredis K., Teichert A., Steitz R., Brems S., Opperdoes B., Van Haesendonck C., Vantomme A., Temst K., The influence of interface roughness on the magnetic properties of exchange biased CoO/Fe thin films, *Journal of Applied Physics,* 107 (11) (2010) 113907.

[18] Jang S. Y., Lim S. H., Lee S. R., Magnetic dead layer in amorphous CoFeB layers with various top and bottom structures, *Journal of Applied Physics,* 107 (9) (2010) 09C707.

[19] Greer A. A., Gray A. X., Kanai S., Kaiser A. M., Ueda S., Yamashita Y., Bordel C., Palsson G., Maejima N., Yang S.-H., Conti G., Kobayashi K., Ikeda S., Matsukura F., Ohno H., Schneider C. M., Kortright J. B., Hellman F., Fadley C. S., Observation of boron diffusion in an annealed Ta/CoFeB/MgO magnetic tunnel junction with standing-wave hard x-ray photoemission, *Applied Physics Letters,* 101 (20) (2012) 202402.

[20] Inyang O., Bouchenoire L., Nicholson B., Tokaç M., Rowan-Robinson R. M., Kinane C. J., Hindmarch A. T., Threshold interface magnetization required to induce magnetic proximity effect, *Physical Review B,* 100 (17) (2019) 174418.